

Structure, Volume 34

Supplemental Information

AlphaFold 3-guided insights into the Importin β : Importin7 heterodimer interaction

and its binding to histone H1

Piotr Neumann, Olexandr Dybkov, Henning Urlaub, Ralf Ficner, and Achim Dickmanns

Supplemental Information

Alphafold 3 guided insights into the Importin β – Importin γ heterodimer interaction and its binding to Histone H1

Piotr Neumann^{1*}, Olexandr Dybkov², Henning Urlaub^{2,3}, Ralf Ficner¹, Achim Dickmanns^{1*#}

¹ Department of Molecular Structural Biology, Institute for Microbiology and Genetics & GZMB, Georg-August-University Göttingen, D-37077 Göttingen

² Bioanalytical Mass Spectrometry Group, Max Planck Institute for Multidisciplinary Sciences, Am Fassberg 11, 37077 Göttingen,

³ Bioanalytics Department of Clinical Chemistry, University Medical Center Göttingen, Göttingen, Germany.

lead contact:

Achim Dickmanns

E-mail: adickma@gwdg.de

*Corresponding authors

Achim Dickmanns

E-mail: adickma@gwdg.de

Piotr Neumann

E-mail: pneuman2@uni-goettingen.de

Figures

FIGURE S1

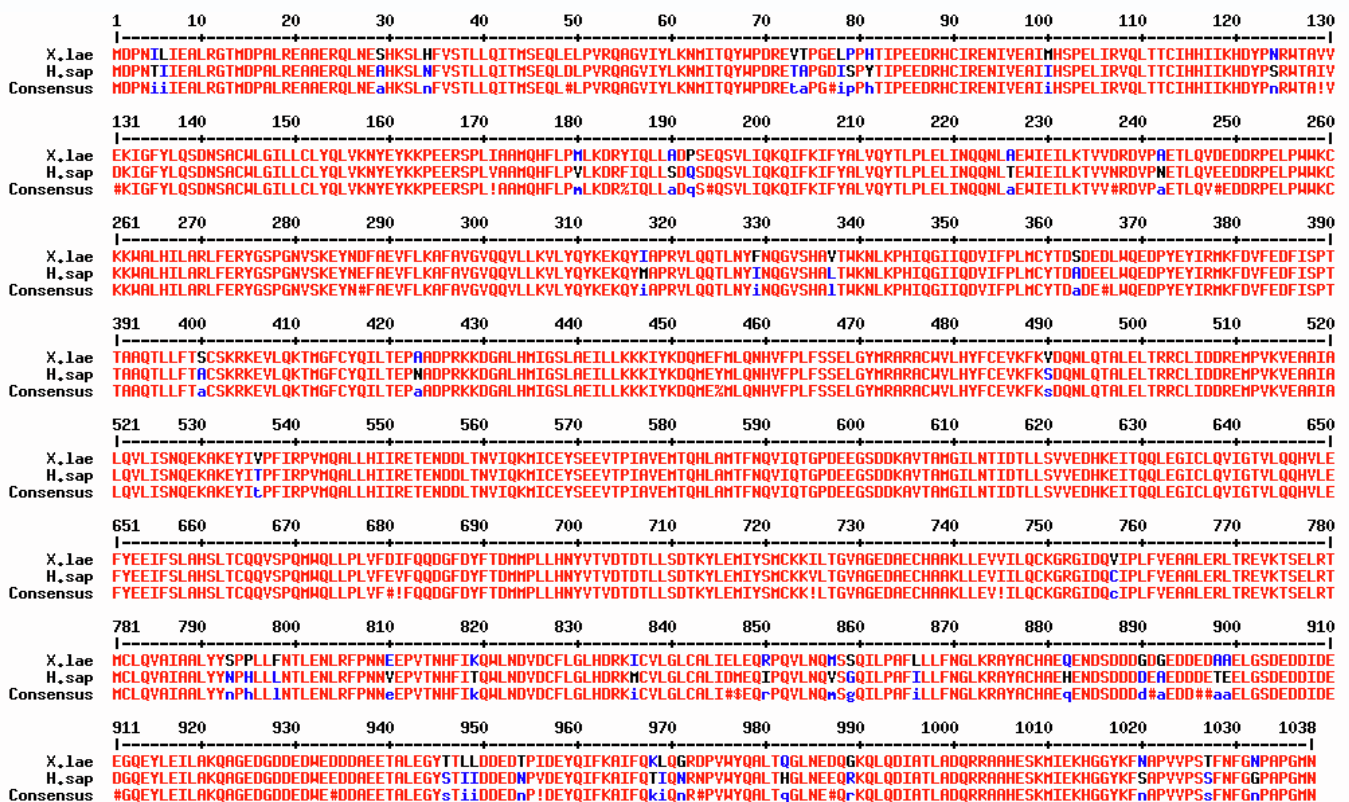


FIGURE S2

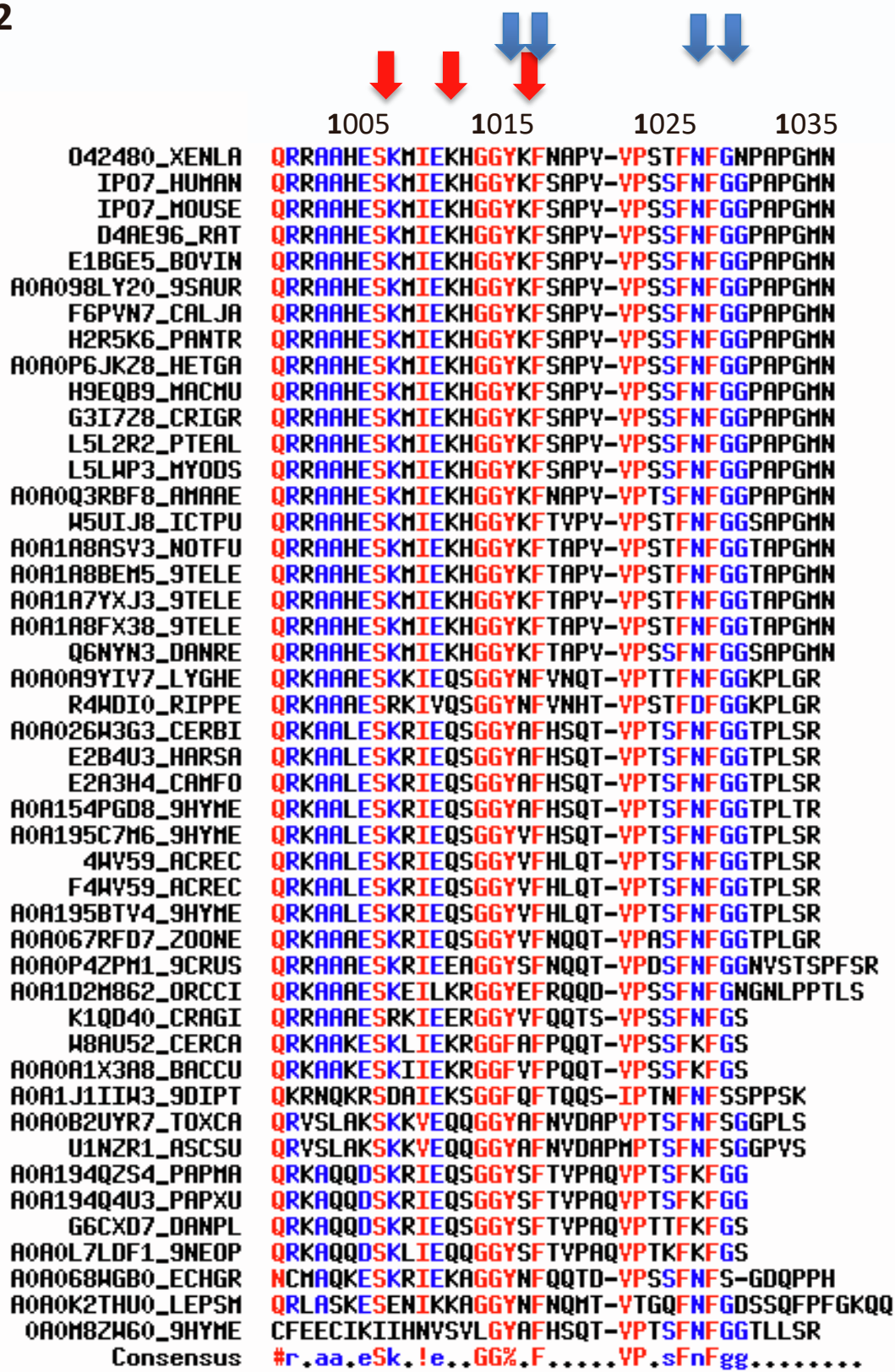


Figure S2: Conservation of NIB (Nucleoporin-like binding) region and indication of the chosen point mutations (Related to Figure 1). Identical residues are marked in red, while highly conserved residues are shown in blue. Conserved lysines presumed essential for function are indicated with red arrows, whereas highly conserved aromatic residues required for binding are marked with blue arrows. Below the alignment, the UniProt references for the Importin 7 sequences used in the alignment are listed. The alignment was performed using MultAlin with standard settings.

Abbreviations for organisms aligned:

O42480_XENLA: *Xenopus laevis* (African clawed frog); IPO7_HUMAN: *Homo sapiens*; IPO7_MOUSE: *Mus musculus*; D4AE96_RAT: *Rattus norvegicus* (norwegian rat); E1BGE5_BOVIN: *Bos Taurus* (cattle); A0A1J1I1W3_9DIPT: *Clunio marinus* (marine midge); F6PVN7_CALJA: *Callithrix jacchus* (White-tufted-ear marmoset); K1QD40_CRAGI: *Crassostrea gigas* (Pacific oyster); A0A0A9YIV7_LYGHE: *Lygus hesperus* (Western plant bug); H2R5K6_PANTR: *Pan troglodytes* (Chimpanzee); W8AU52_CERCA: *Ceratitis capitata* (Mediterranean fruit fly); A0A0B2UYR7_TOXCA: *Toxocara canis* (Canine roundworm); A0A0A1X3A8_BACCU: *Bactrocera cucurbitae* (Melon fruit fly); A0A0P4ZPM1_9CRUS: *Daphnia magna* (Big water flea); A0A026W3G3_CERBI: *Cerapachys biroi* (Ant); E2B4U3_HARSA: *Harpegnathos saltator* (Jerdon's jumping ant); A0A0P6JKZ8_HETGA: *Heterocephalus glaber* (Naked mole rat); W5UIJ8 ICTPU: *Ictalurus punctatus* (Channel catfish); H9EQB9_MACMU: *Macaca mulatta* (Rhesus macaque); Q6NYN3_DANRE: *Danio rerio* (Zebrafish); A0A068WGB0_ECHGR: *Echinococcus granulosus* (Hydatid tapeworm); R4WDI0_RIPPE: *Riptortus pedestris* (Bean bug); 4WV59_ACREC: *Acromyrmex echinator* (Panamanian leafcutter ant); A0A194Q4U3_PAPXU: *Papilio xuthus* (Asian swallowtail butterfly); G6CXD7_DANPL: *Danaus plexippus* (Monarch butterfly); G3I7Z8_CRIGR: *Cricetulus griseus* (Chinese hamster); R4WDI0_RIPPE: *Riptortus pedestris* (Bean bug); A0A194QZS4_PAPMA: *Papilio machaon* (Old World swallowtail); F4WV59_ACREC: *Acromyrmex echinator* (Panamanian leafcutter ant); A0A067RFD7_ZOONE: *Zootermopsis nevadensis* (Dampwood termite); L5L2R2_PTEAL: *Pteropus alecto* (Black flying fox); E2A3H4_CAMFO: *Camponotus floridanus* (Florida carpenter ant); A0A154PGD8_9HYME: *Dufourea novaeangliae* (sweet bee); L5LWP3_MYODS: *Myotis davidii* (David's myotis); A0A0Q3RBF8_AMAAE: *Amazona aestiva* (Blue-fronted Amazon parrot); A0A195BTV4_9HYME: *Atta colombica* (leafcutter ant); A0A0L7LDF1_9NEOP: *Operophtera brumata* (winter moth); A0A195C7M6_9HYME: *Cyphomyrmex costatus* (Fungus-growing ant); A0A1D2M862_ORCCI: *Orchesella cincta* (Springtail); U1NZR1_ASCSU: *Ascaris suum* (Pig roundworm); A0A098LY20_9SAUR: *Hypsiglena sp.* JMG-2014 (Nightsnake); A0A1A8ASV3_NOTFU: *Nothobranchius furzeri* (Turquoise killifish); A0A0K2THU0_LEPSM: *Lepeophtheirus salmonis* (Salmon louse); A0A1A8BEM5_9TELE: *Nothobranchius kadlecii* (Kadlec's killifish); A0A1A7YXJ3_9TELE: *Aphyosemion striatum* (Red-striped Killifish); A0A1A8FX38_9TELE: *Nothobranchius korthausae* (Kinungamkele red tail killifish).

(Multiple sequence alignment with hierarchical clustering; F. CORPET, 1988, Nucl. Acids Res., 16 (22), 10881-10890).

FIGURE S3

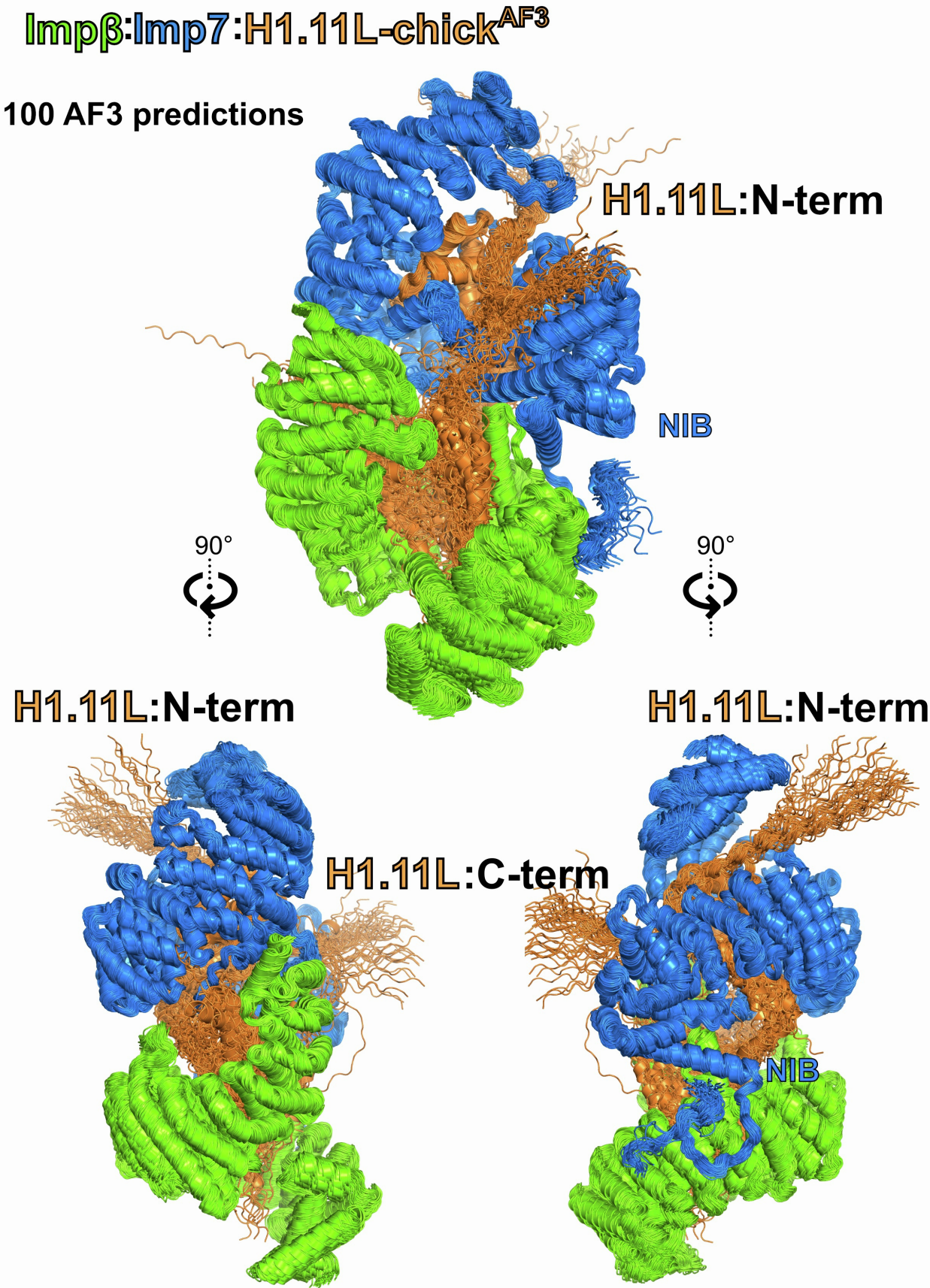


Figure S3: AF3-modelling fitted the H1 core into Imp7 and the H1-Lys rich flexible regions within Imp β (Related to Figure 1B). Interestingly, the termini predominantly exit the central cavity by interactions localized on Imp7.

FIGURE S5

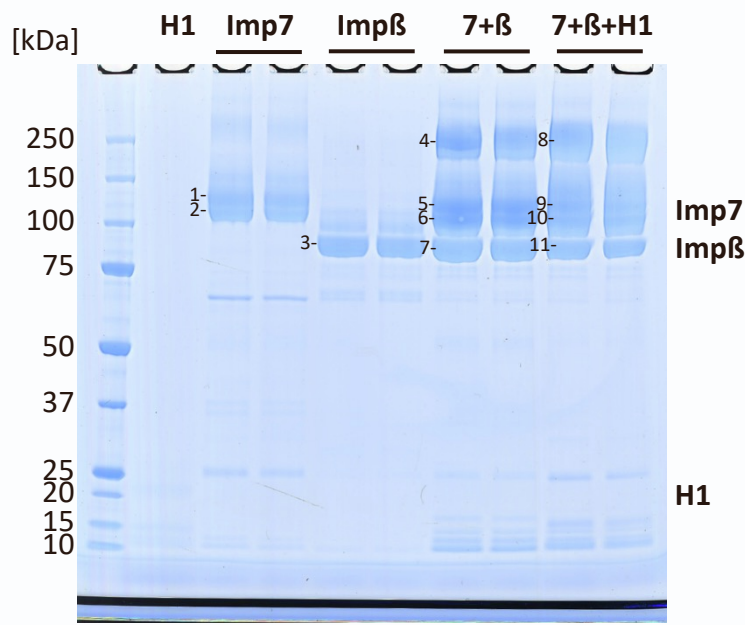


Figure S5: SDS-polyacrylamide gel of BS3-cross-linked histone 1.11L, importin 7 and importin β and complexes thereof (Related to Figure 2, Table S3). xlImp7, hsImp β and ggH1.11L, purified as described in Wohlwend et al.³⁶, were subjected to protein-protein cross-linking mass spectrometric analysis (CXMS) as described in main text materials and methods section. The BS3-cross-linked proteins and complexes thereof were separated using SDS-PAGE and visualized by Coomassie staining. The numbered bands were excised and analyzed by CXMS. See Table S3 for detailed results.

FIGURE S6

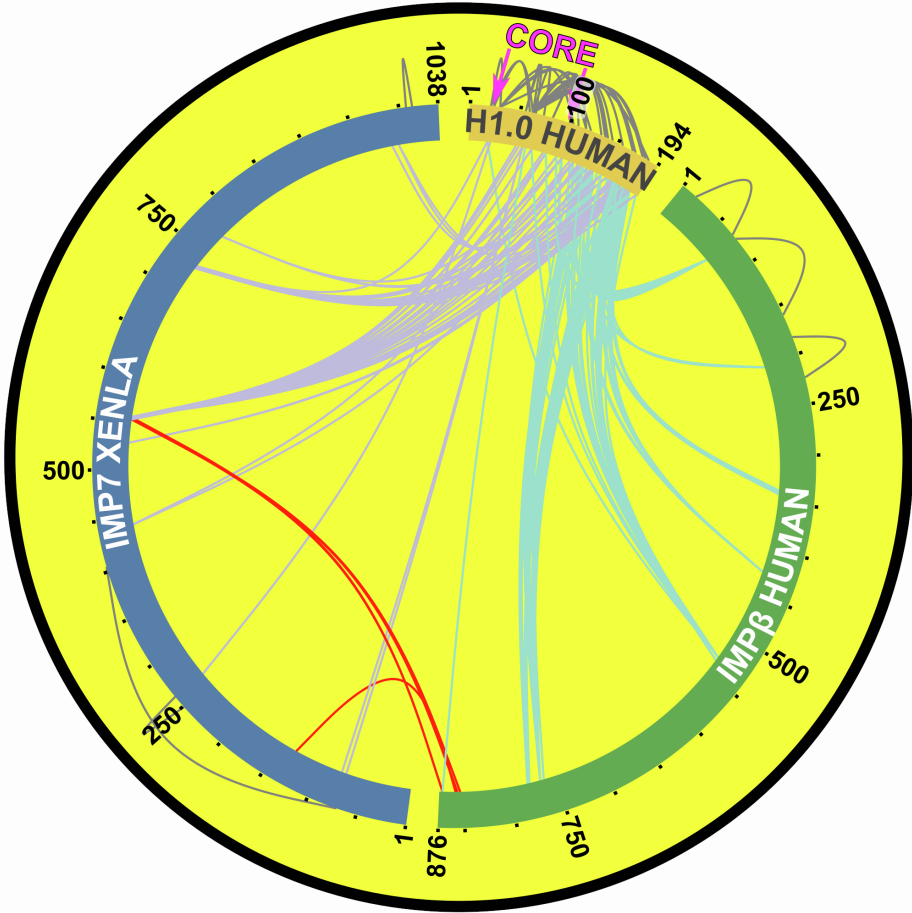


Fig. S6. Cross-linking experiments confirm the structural models generated by AlphaFold 3 (AF3) (Related to Figure 2). Imp7 is depicted in blue, Impβ in green and H1 in yellow-orange. Impβ:Imp7:H1.0-hs DMTMM data taken from Ivic et al 2019. Upper left panel: Proteins indicated as bars in a circular plot created with xiVIEW, with cross-links shown in red for Imp7-Impβ, Violet for Imp7-H1 and Cyan for H1-Impβ.

FIGURE S7

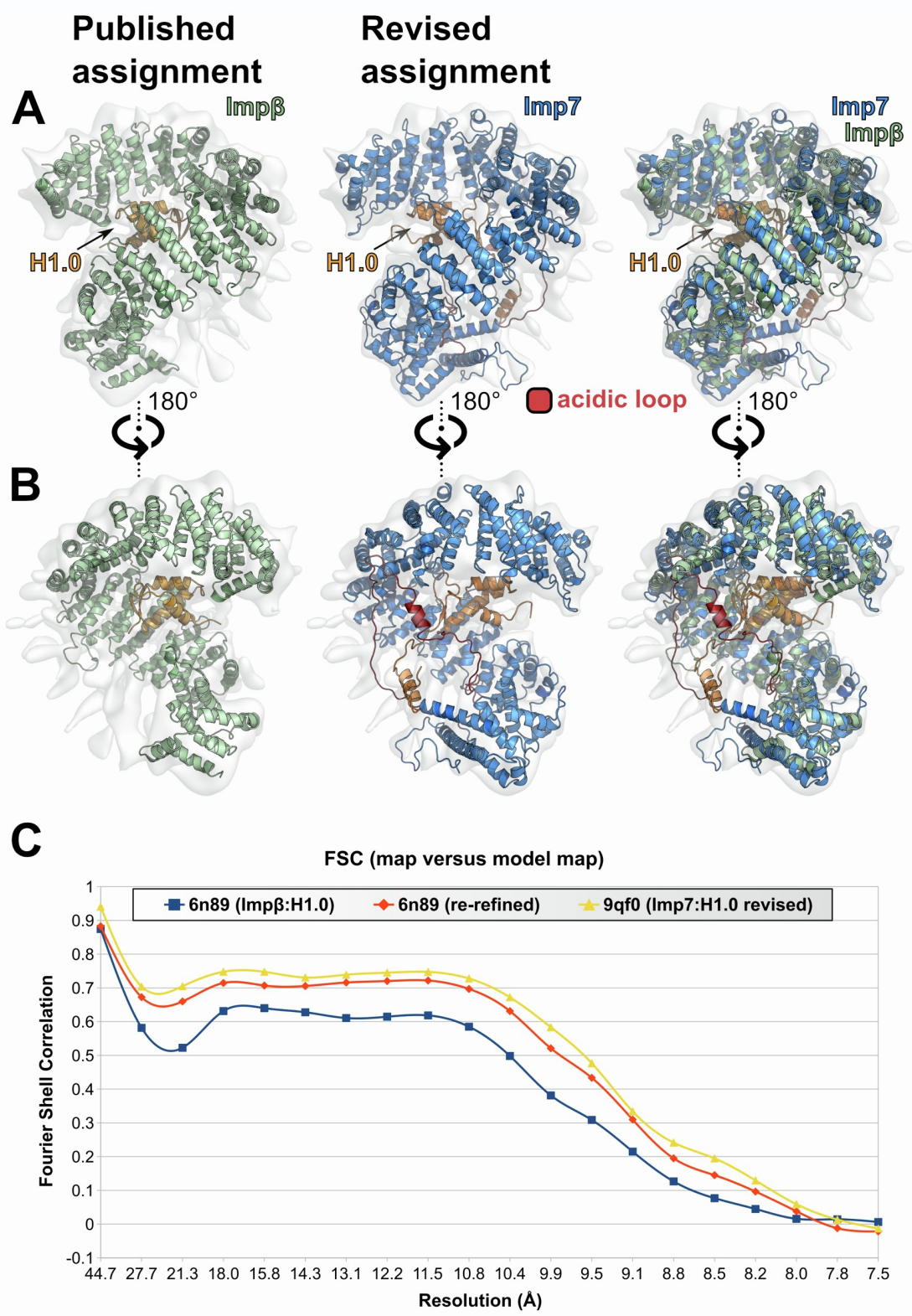


Figure S7: Comparison of the model to map correspondence between the revised *Imp7*:H1 complex and the original interpretation (*Impβ*:H1 structure) (Related to Figure 3). **A.** Panels from left to right: *Impβ*:H1 (PDBid: 6N89), *Imp7*:H1 and overlay of both. In each case the map (EMDBid: 0367) is shown in light gray. **B.** 180° turn of the orientation in A. **C.** The FSC curves calculated for compared structural models: *Impβ*:H1, a re-refined version of *Impβ*:H1 (as described in main text materials and methods section) and the *Imp7*:H1 based on the AF3 model.

FIGURE S8

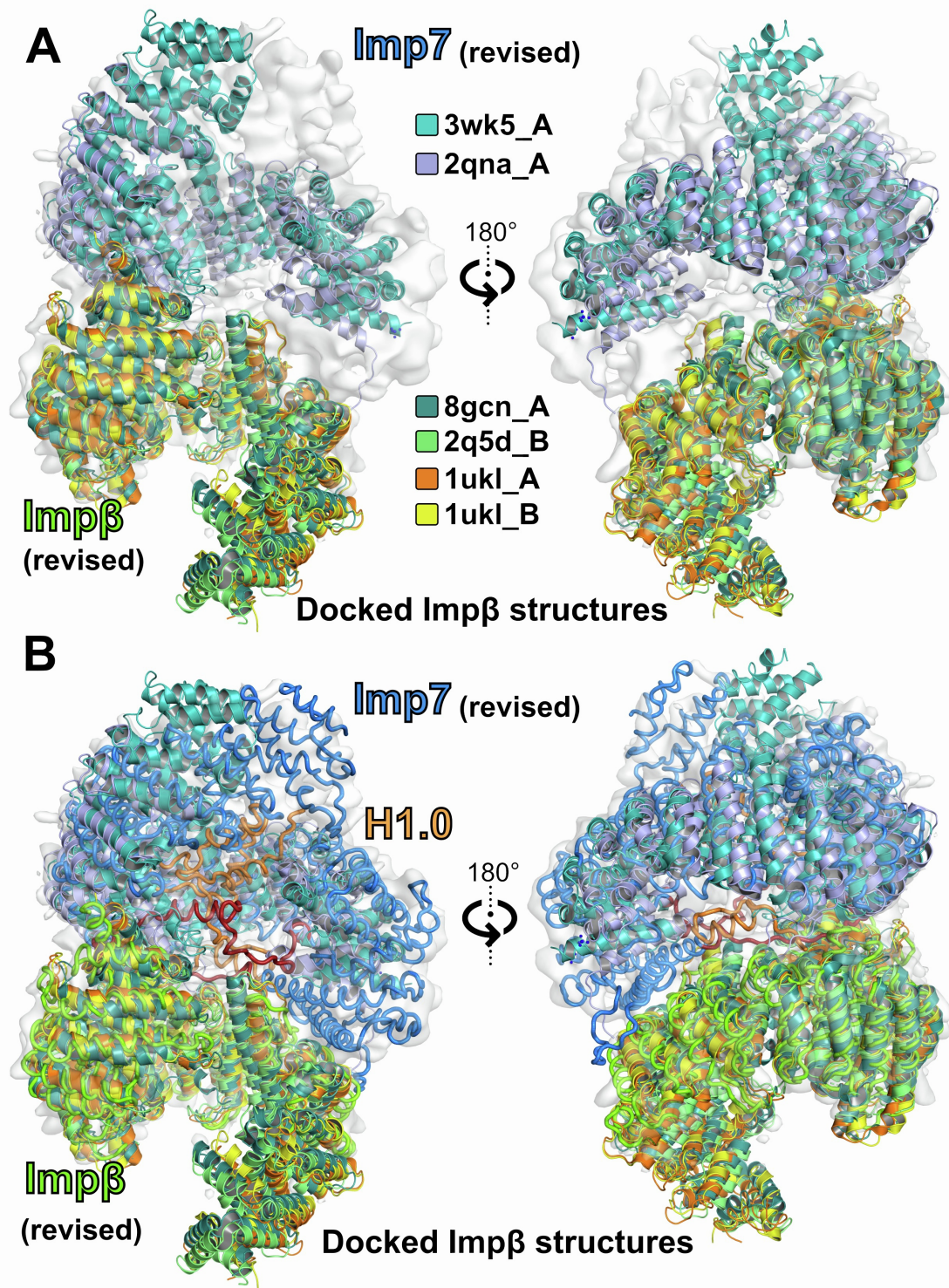


Figure S8: Deposited crystal structures of Impβ were used for automated placement into the EM-map (Related to Figure 3). The phenix.dock_in_map program to dock full-length Impβ crystal structures into the cryo-EM map (EMD-0366) revealed a striking observation: four models (PDB IDs_chain-id: 1ukl_A, 1ukl_B, 2q5d_B, 8gcn_A) were unequivocally placed in the region previously misassigned as Imp7. In contrast, two Impβ structures: 2qna_A (bound to the IBB domain of Snurportin1) and 3w5k_A (bound to the C2H2 zinc-finger protein SNAIL1), aligned with the incorrect assignment, highlighting the importance of rigorous structural validation.

FIGURE S9

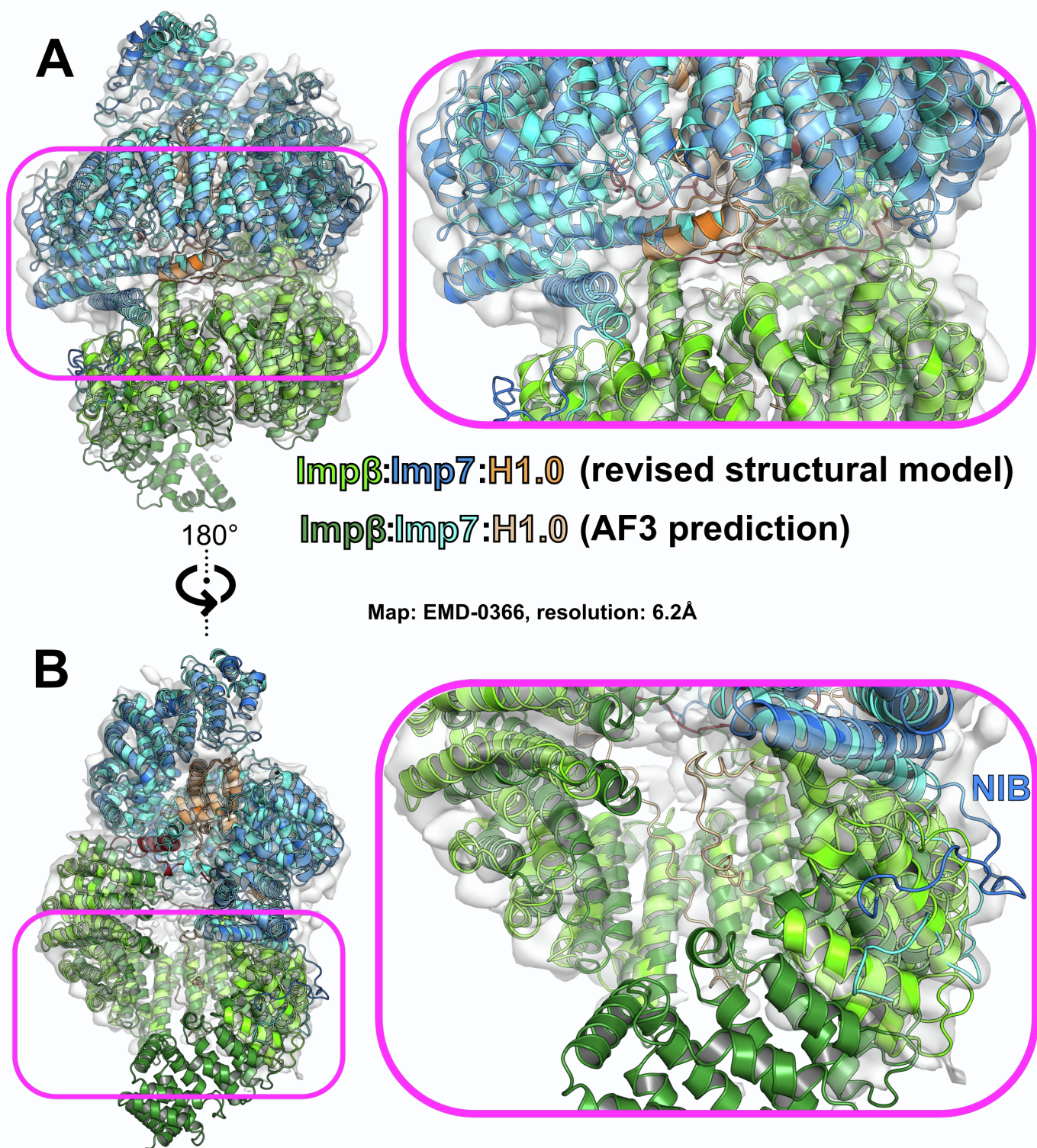


Figure S9: Comparison of the AF3 generated model of Impβ:Imp7:H1 and the refined structural model (Related to Figure 3). **A.** Overall structure of the ternary complex (left) and magnification of the boxed region (right) reveals only subtle changes at the interface of the three proteins. In contrast, in **B.** is presented the 180° rotational view (right) and the magnification of the NIB region and its binding site, which are more compact in the structural model. Coloring of the individual proteins as indicated in the figure.

FIGURE S10

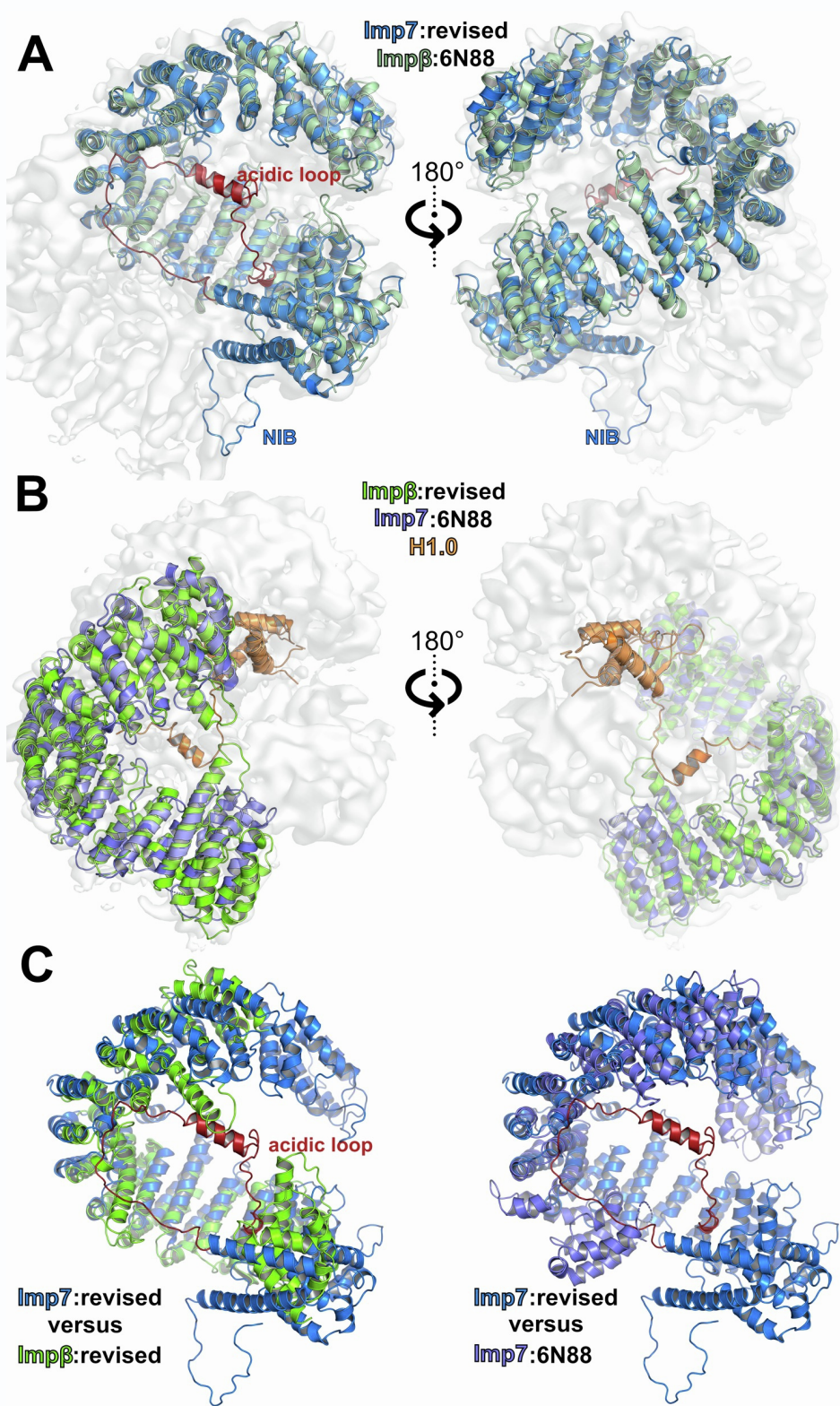


Figure S10: Comparison of the Imp7:Impβ:H1 complex (6N88) and the revised structural model Impβ:Imp7:H1 against the cryo-EM map (EMDB-0366) (Related to Figure 3). **A.** Superposition of the respective molecules positioned in the upper part of the map in two orientations. **B.** Superposition of the respective molecules positioned in the lower part of the map in two orientations. **C.** The overlay of Imp7 and Impβ of the revised structure (left panel) as well as the overlay of Imp7 of the revised structure and Imp7 from 6N88 (right panel) exhibit a similar curvature and arrangement in the middle region, but distinct differences C- and N-terminal regions.

FIGURE S11

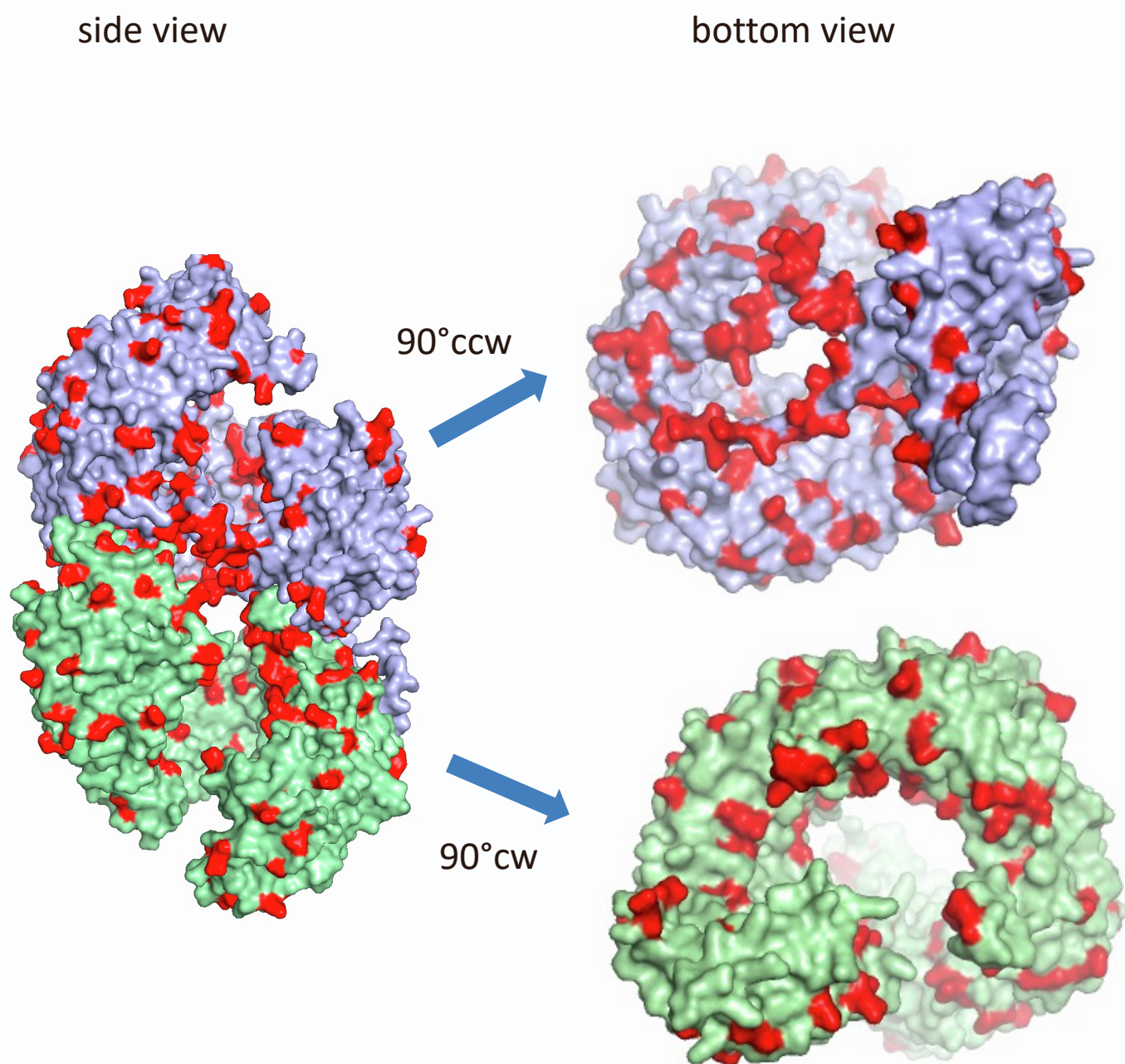
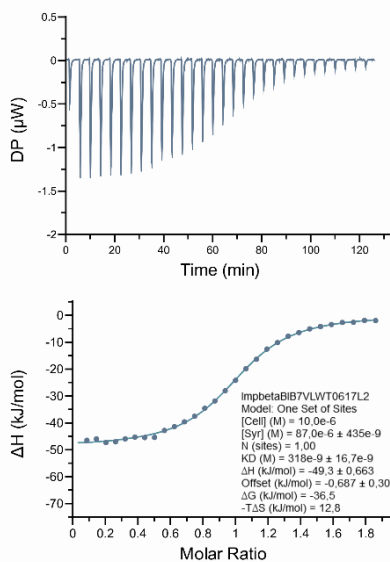


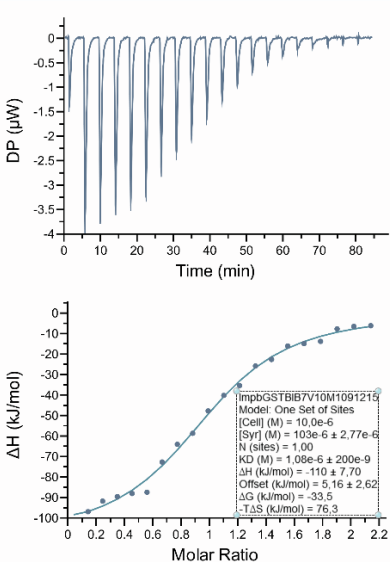
Figure S11: Importin 7 is rich in acidic residues on the inner surface. (Related to Figure 3). **Left:** The complex of Imp β (green) and Ipo7 (light violet) are depicted with the acidic residues colored in red. **Right:** The individual molecules are rotated by 90 degrees so that the inner surface can be seen from the bottom. ccw: counter clockwise , cw: clockwise rotation.

FIGURE S12

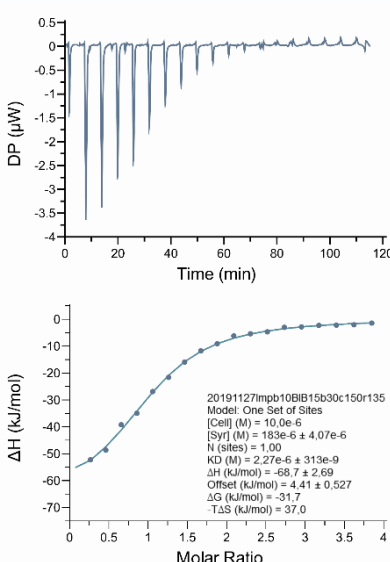
1002-1038 wt



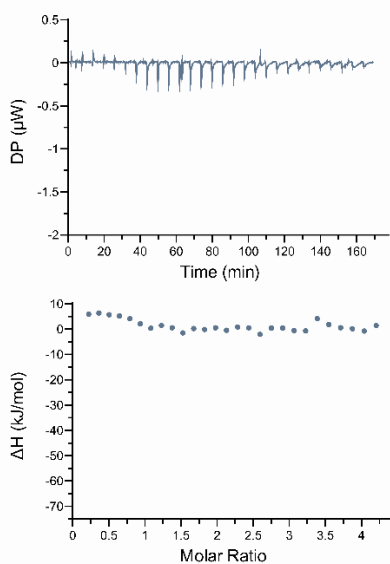
1015-1033



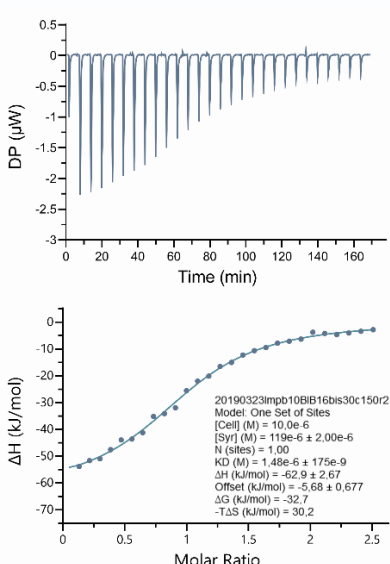
1015-1030



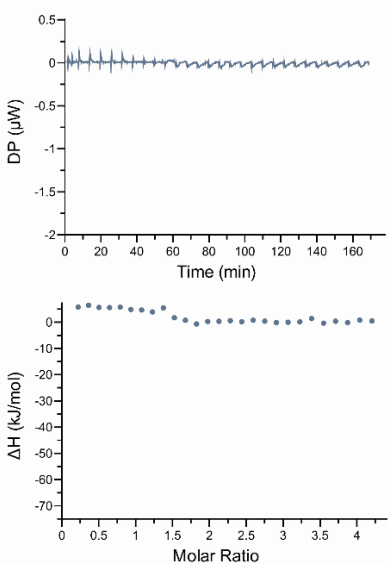
1015-1029



1016-1030



1017-1029



1015-1029 buffer control

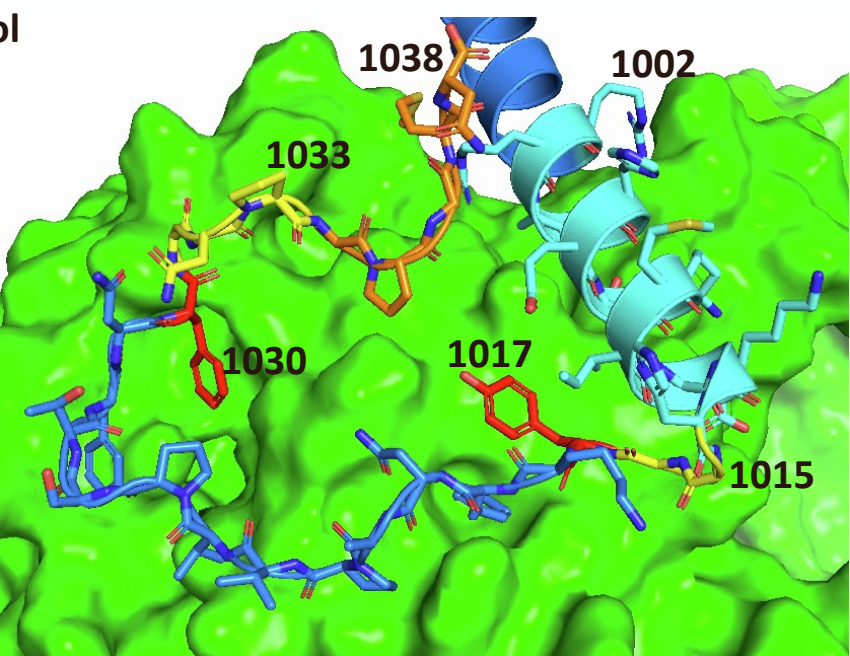
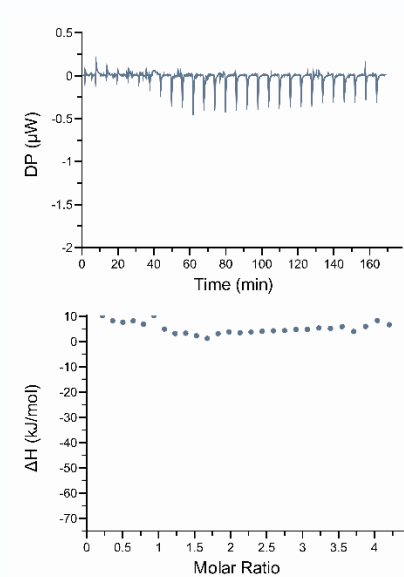
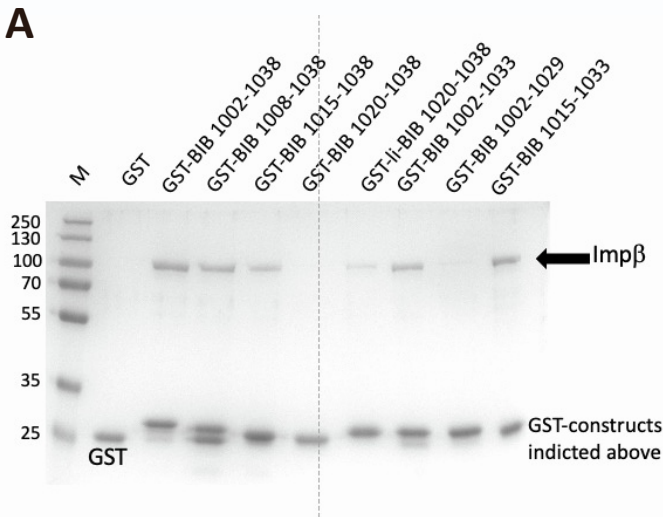


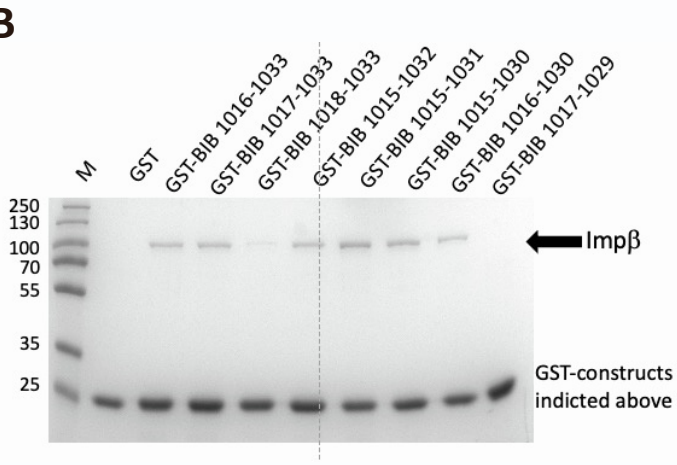
Figure S12: ITC results of the tested deletion mutants reveal the requirement of residues 1016-1030 for binding to Imp β (Related to Table 1). The thermograms and data evaluation of representative experiments, selected to be close to the average values reported in Table 1 of the main text, are shown. The results for the deletion constructs are shown, with the numbers above indicating the regions expressed as GST-fusion proteins. These fusion proteins contain a PreScission Protease cleavage site and an additional GS dipeptide due to the restriction site used for cloning, positioned before the actual first residue of the NIB-region in order to improve accessibility. The bottom right panel depicts the complete NIB-region starting at residue 1002 (cyan). Yellow residues highlight the GG-pair marking the beginning of the flexible tail region of the NIB-region, as well as C-terminal residues that could be deleted. The stretch shown in blue, flanked by red aromatic residues, represents the required region for binding to Imp β . Additionally, before unpredicted residues from the preceding α -helix are depicted in blue.

FIGURE S13

A



B



C

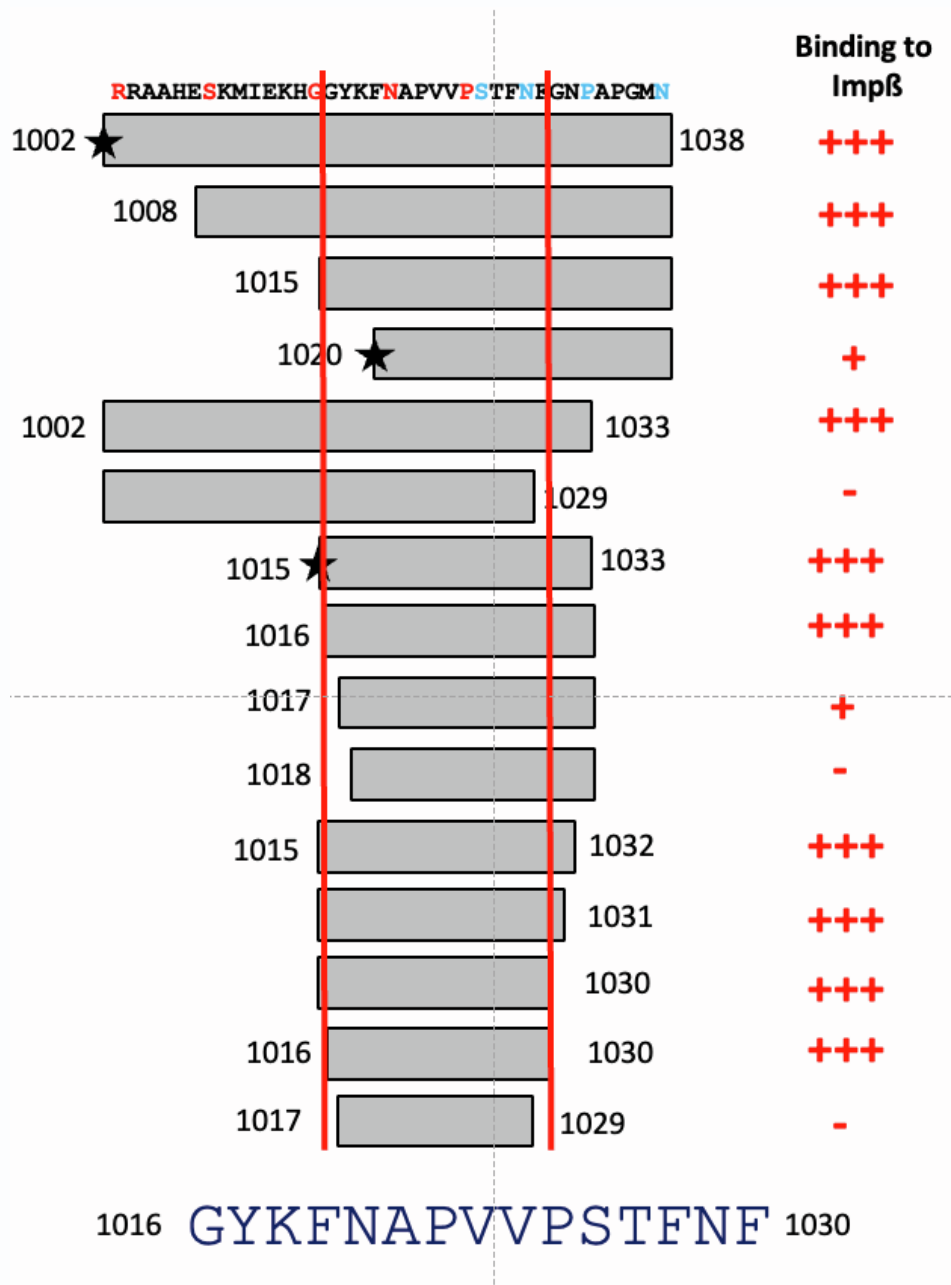


Figure S13: Pull down experiments confirm the results obtained from deletions tested in the ITC experiments (Related to Table 1). **A.** Pulldown experiments were performed as described, analyzed by SDS-PAGE chromatography and visualized by Coomassie staining. Deletion mutants of the NIB-domain were constructed resulting in GST-fused fragments, expressed, purified (M&M) and used in pull-down experiments with Imp β (for a comprehensive list see Table. S1). Deletion of the first six residues (NIB1008-1038; the deletion mutant form used in (Bäuerle, 2002) did not alter the binding properties, neither did the deletion of the next seven residues from the N-terminus (NIB1015 – 1038). In contrast, further deletion by the next five or ten residues abrogated binding of Imp β . From the C-terminal end, only the deletion of the last five residues (NIB1002-1033) did not compromise Imp β binding, whereas further deletions (NIB1002-1029, NIB1002-1026) abolished binding completely. A fragment with residue 1033 at the C-terminus and different deletions from the N-terminal side resulted in the expected fragment comprising residues 1015 to 1033 (NIB1015-1033), which is still able to interact with Imp β in pull down experiments. Further deletions revealed that 1016-1030 still binds to Imp β , whereas shorter versions (NIB1020-1033, NIB1025-1033) did not bind anymore. In order to exclude spatial restraints between the GST-moiety and the NIB-fragment as reason for a lack of binding, a 15-residue linker (see M&M in main text) was introduced in some fragments to extend the distance between GST and the NIB fragment. The resulting proteins were also tested and exhibited the same properties as the ones without the linker (Fig. 11C indicated by a star), excluding the possibility of spatial restraints as reason for non-binding to Imp β . **B.** In a second round, deletions fragments of Imp7 were cloned, expressed and used in pull-down experiments, that were shortened by steps of one residue either from the N or C-terminal side starting at 1015 and 1033, respectively. Deletion of residues 1015 from the N-terminus or three residues (down to G1031) from the C-terminus did not alter the binding properties significantly (Fig. 1B). As soon as residues 1016 or 1030 (mutant NIB 1017-1029) were removed the binding dramatically decreased. So, it can be concluded, that the minimal binding region lies within residues 1016 to 1030 of Imp7. **C.** Qualitative summary of the deletion experiments.

FIGURE S14

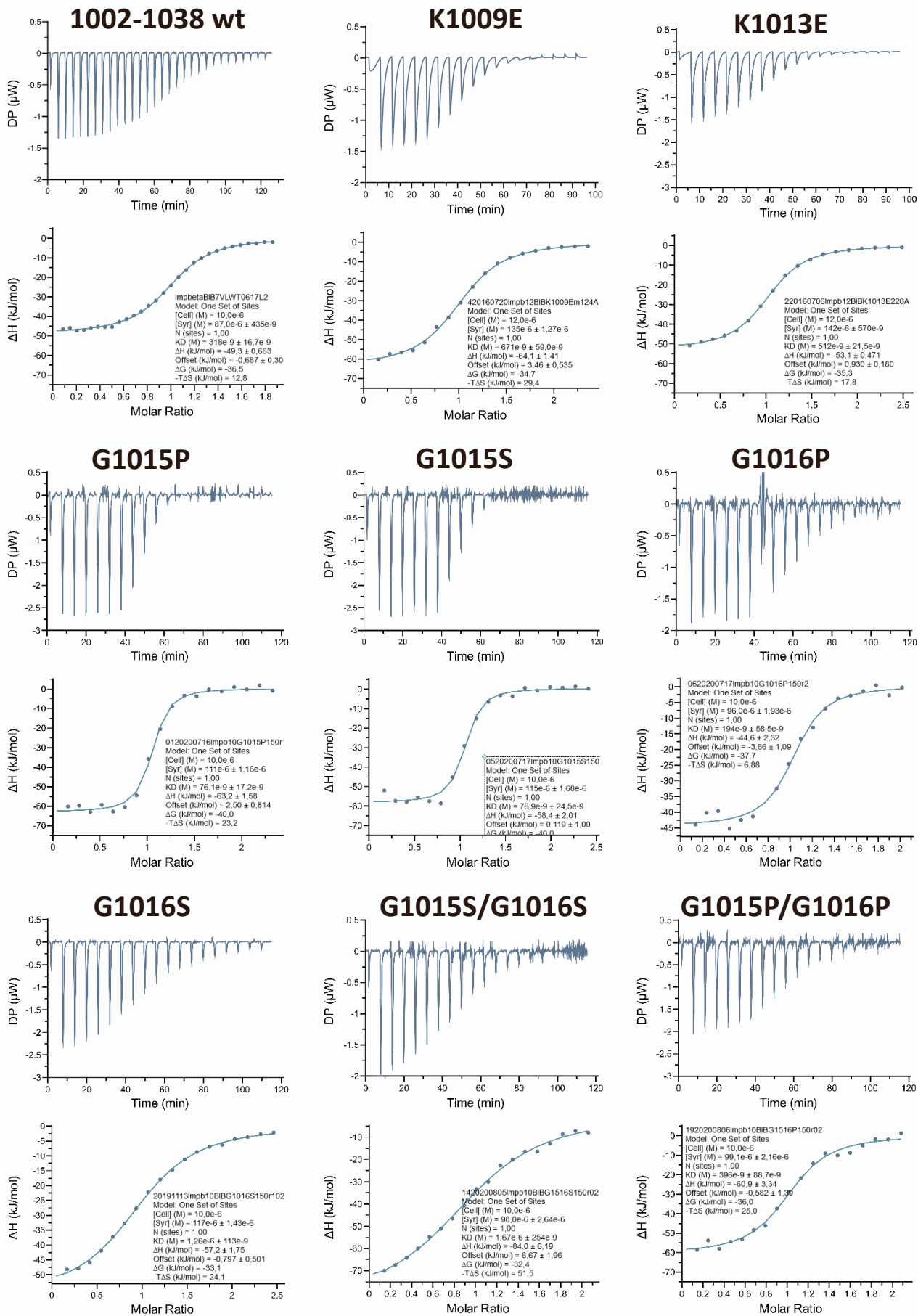


Figure S14: The ITC results of the tested point mutations are presented (Related to Figure 5). The thermograms and data evaluation of representative experiments, selected to be close to the average values reported in Table S7, are shown. Lysine residues (see also S15) within the NIB region, as well as the GG pair preceding the intrinsically disordered region (IDR), do not play a significant role in binding to Imp β , contrary to earlier speculations.

FIGURE S15

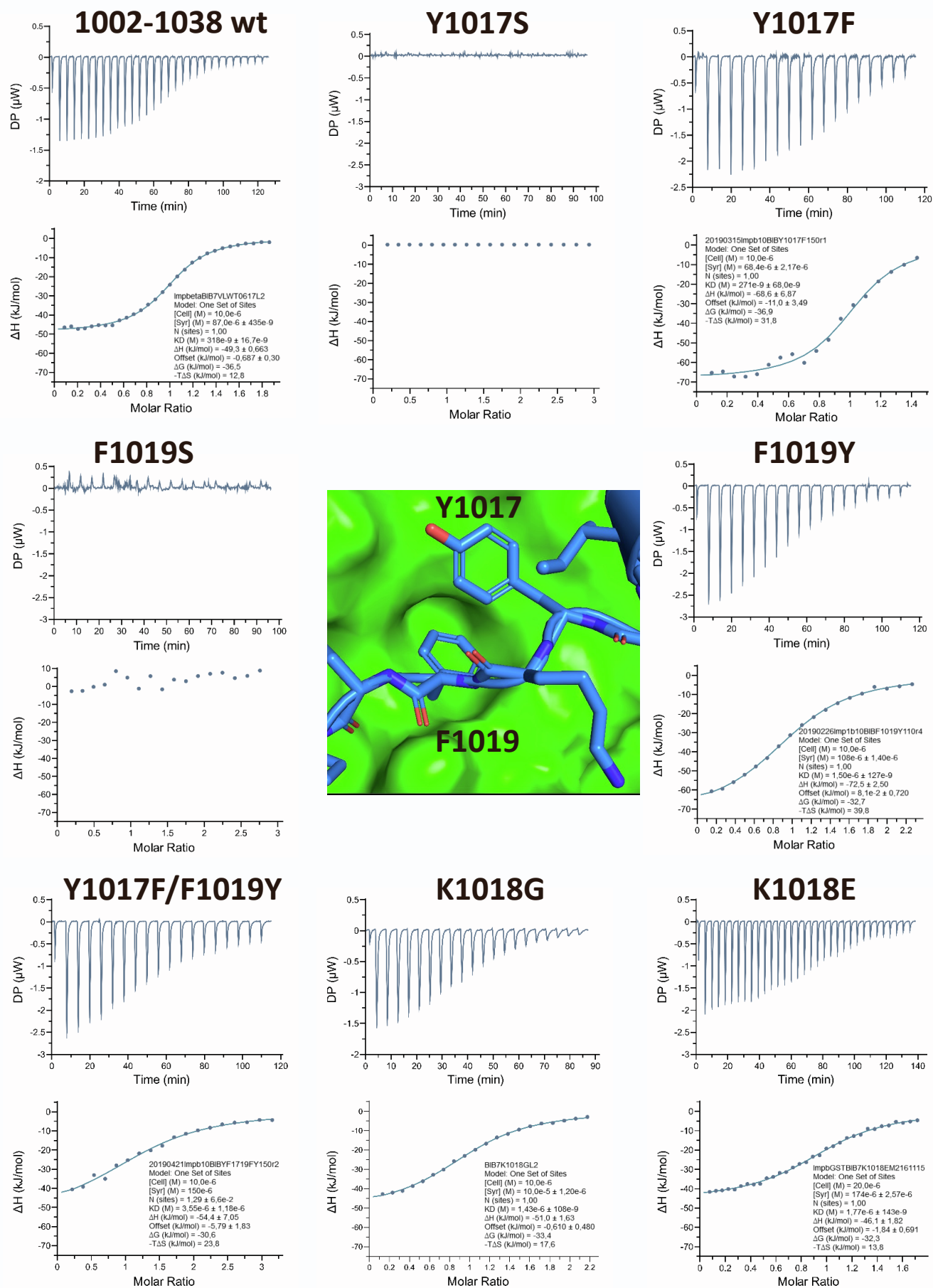


Figure S15: The ITC results of the tested point mutations are presented (Related to Figure 5). The thermograms and data evaluation of representative experiments, selected to be close to the average values reported in Table S7, are shown. The first binding motif, YxF at positions 1017 and 1019, is required and essential for binding. However, either Y or F at both positions is sufficient to secure binding. The central image illustrates the binding mode.

FIGURE S16

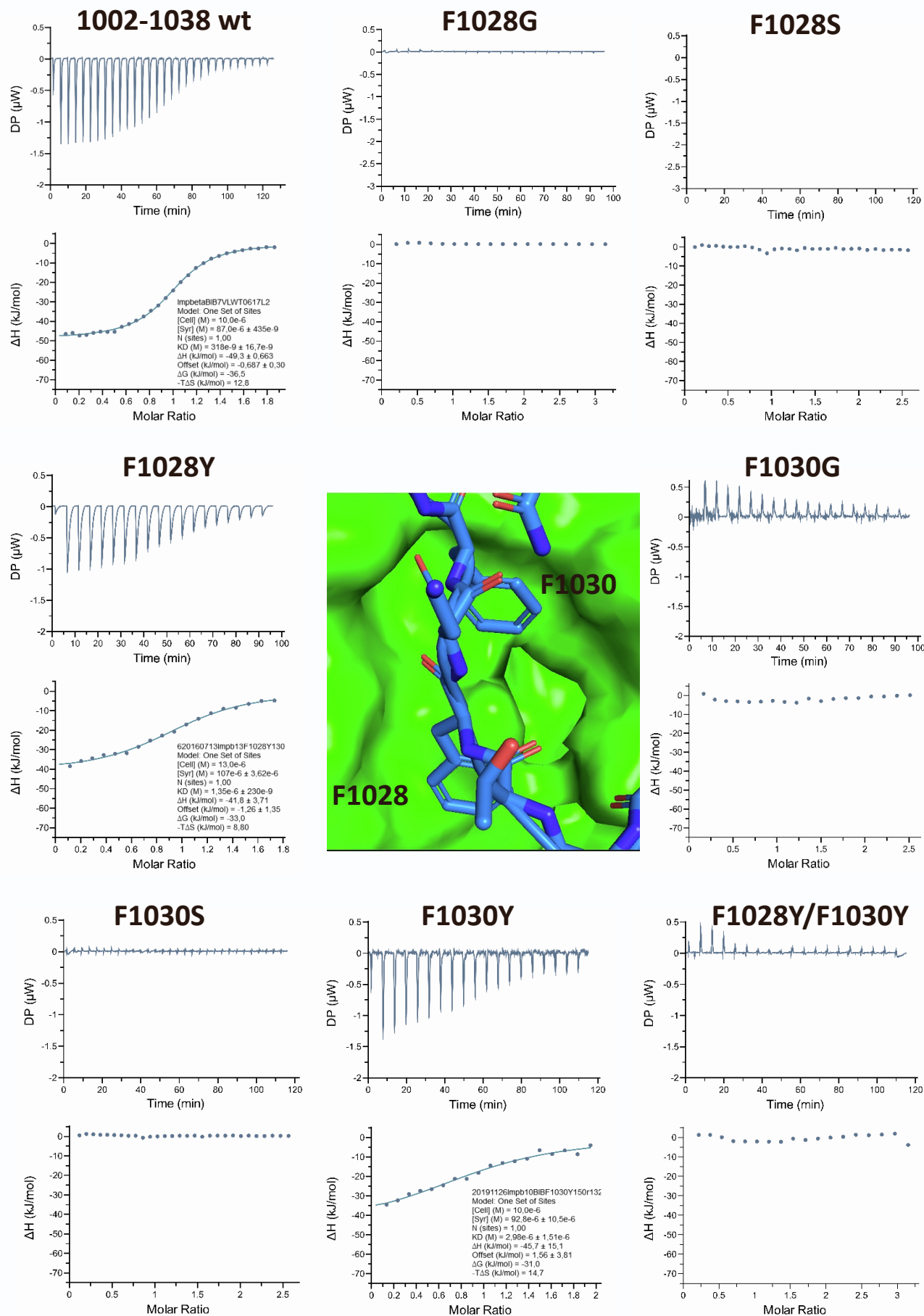


Figure S16: The ITC results of the tested point mutations are presented (Related to Figure 5). The thermograms and data evaluation of representative experiments, selected to be close to the average values reported in Table S7, are shown. The second binding site, FxF, is required and essential for binding. At most, only one F residue may be substituted with Y at a time to retain binding. The central image illustrates the binding mode.

FIGURE S17

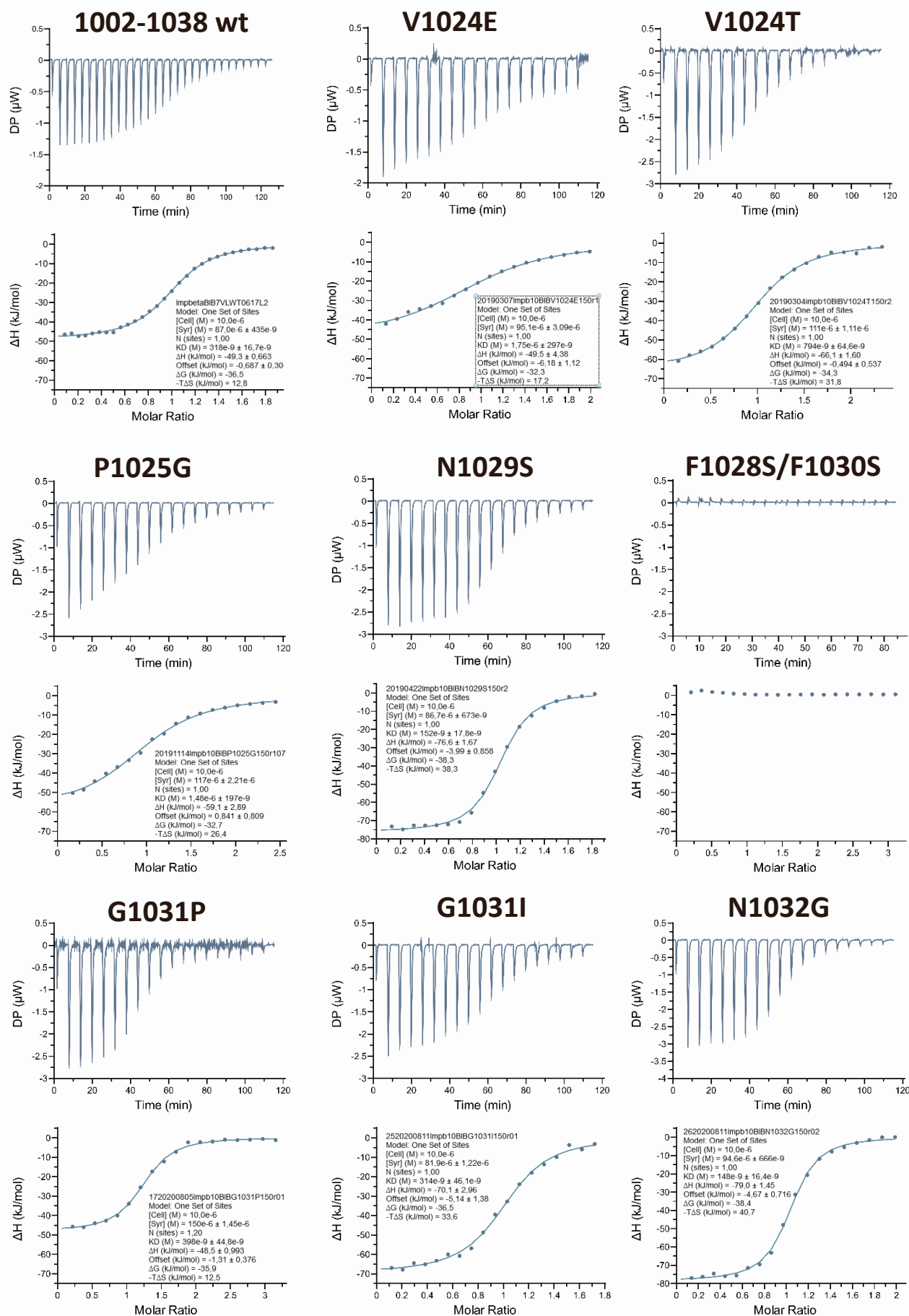


Figure S17: The ITC results of the tested point mutations are presented (Related to Figure 5). The thermograms and data evaluation of representative experiments, selected to be close to the average values reported in Table S7, are shown. The remaining conserved residues (Fig. S2) affect the binding affinity but do not completely abolish the interaction between the NIB region and Imp β .

FIGURE S18

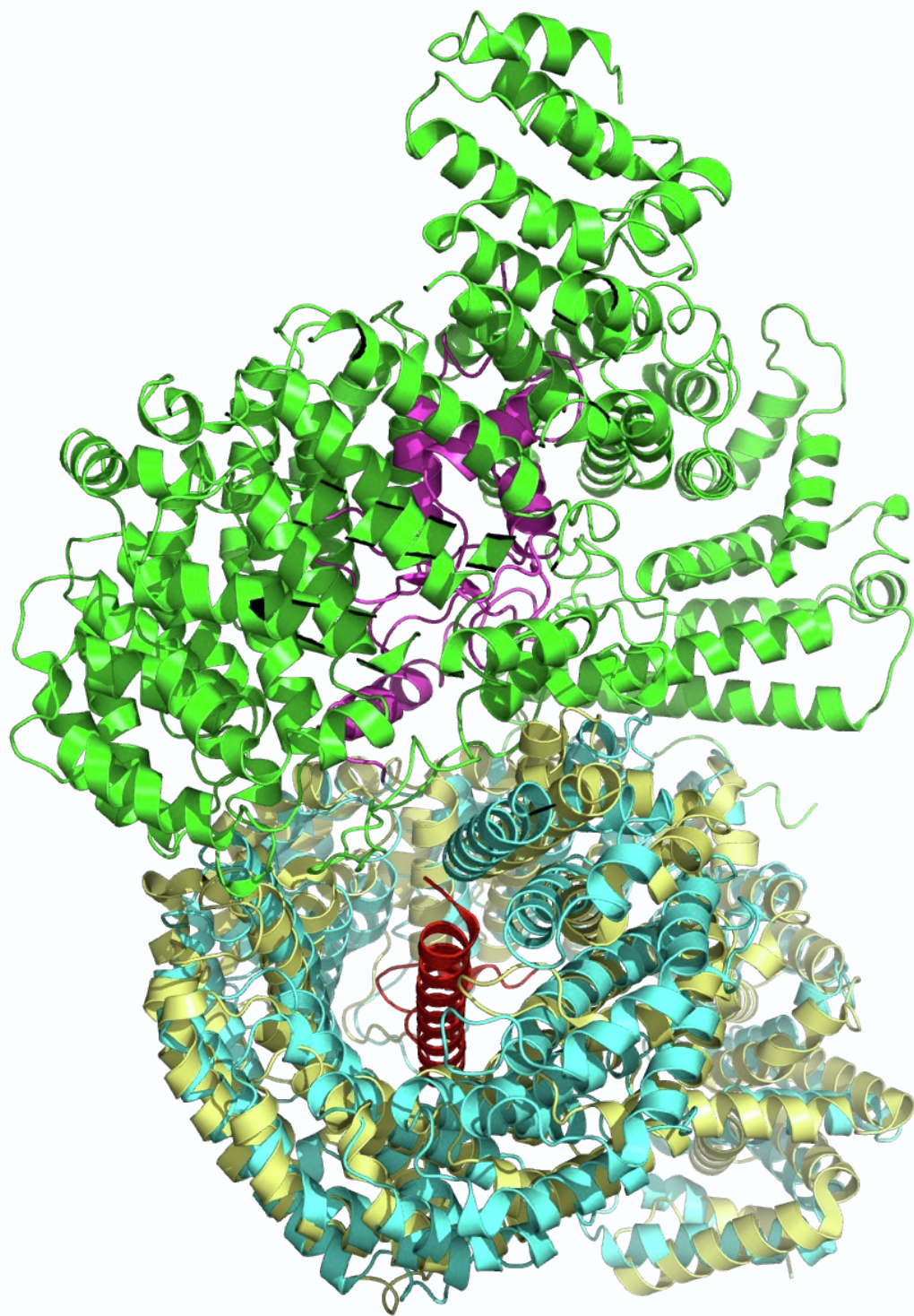


Figure S18: The Imp β :Imp7:H1 complex is still able to interact with the IBB domain of Imp α (Related to Figure 1). The structure of Imp β :Imp α -IBB (PDBid: 8gcn) was superposed to Imp β of the ternary complex. Binding of H1 and Imp α -IBB do not interfere with each other in this arrangement, as shown experimentally by Jäkel et al. (Jäkel, S. et al. The Importin β /Importin 7 Heterodimer Is a Functional Nuclear Import Receptor for Histone H1. The EMBO Journal vol. 18 <https://www.embopress.org> (1999))

FIGURE S19

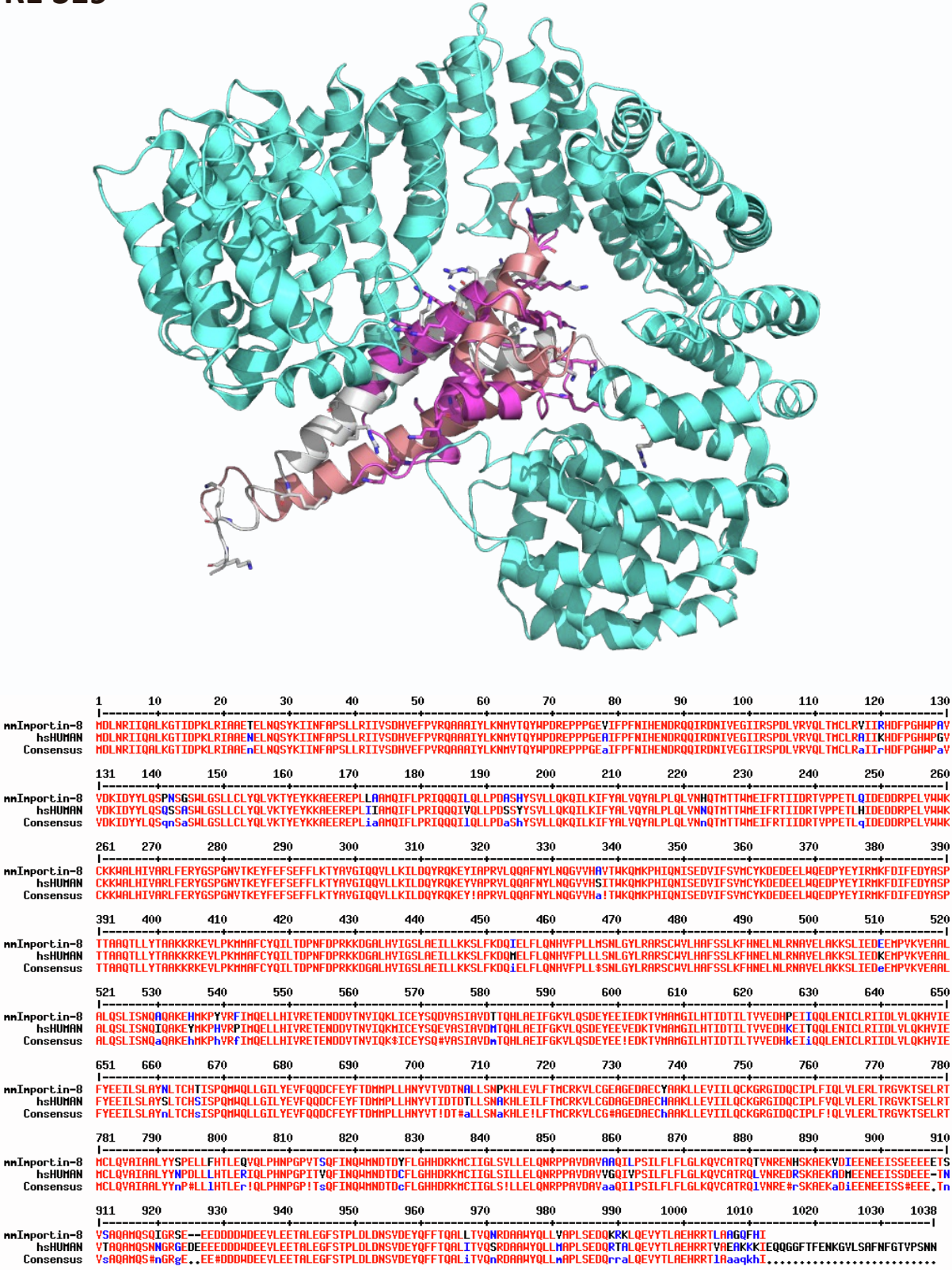


FIGURE S20

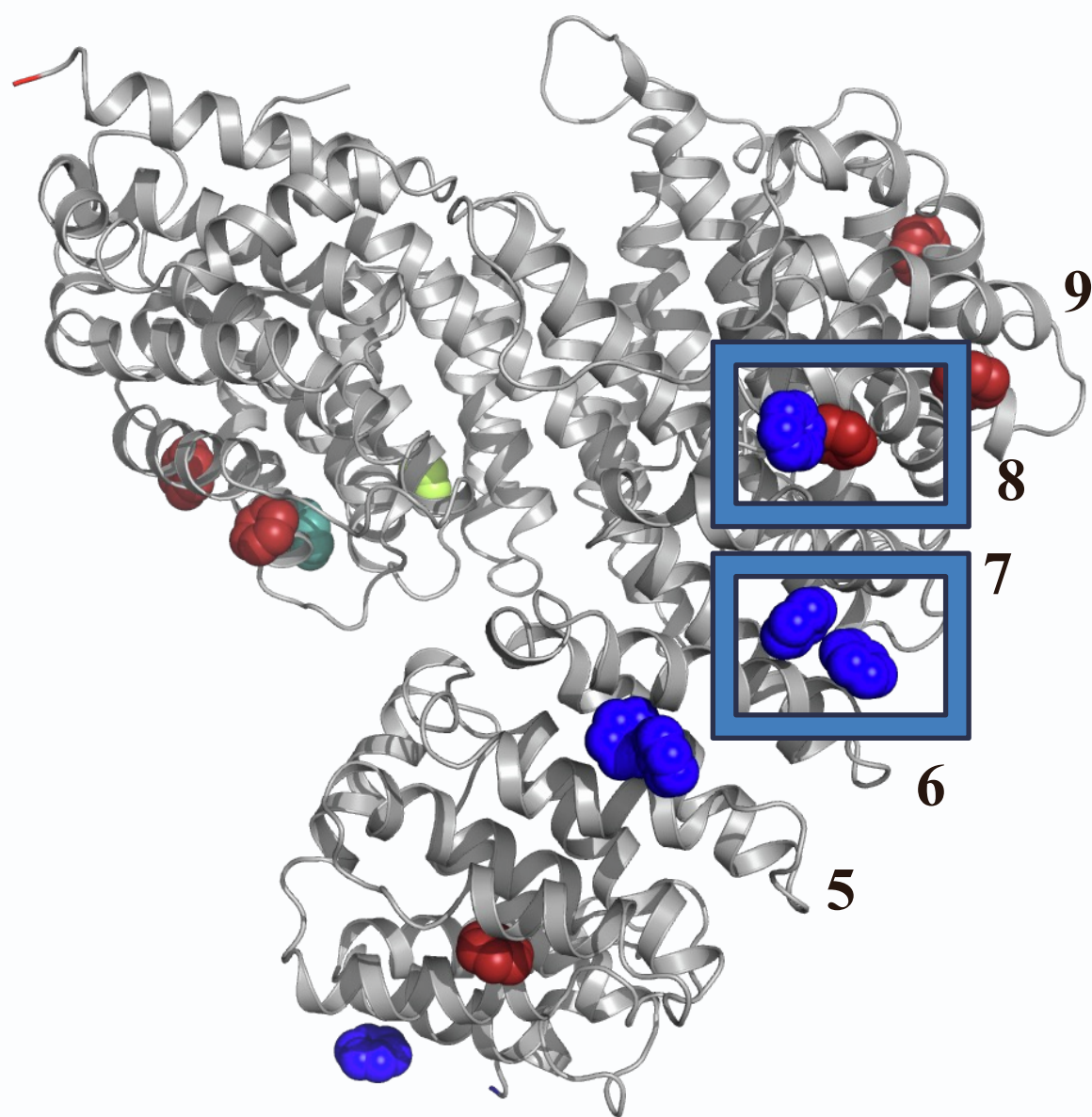


Figure S20: Experimentally (X-Ray and biochemically) defined as well as *in silico* predicted FG binding sites on the surface of Impβ (Related to Figure 5). The coloring indicates the following: Blue: found in crystal structures, Dark red: found by *in silico* simulation, Green: biochemically determined, Limon: both *in silico* and biochemically. The numbering indicates the A helices of the HEAT repeats forming the respective cleft for NIB region binding.

Tables

Table S1: Primers used to create deletions. Related to STAR Methods.

pGEX BIB ₇ 1002_for	CCGGATCCATGAGGCGGGCAGCACATGAATCC
pGEX BIB ₇ 1008_for	CCGGATCCATGTCCAAAATGATCGAGAAACAC
pGEX BIB ₇ 1015_for	CCGGATCCATGGGAGGCTACAAATTCAACGCC
pGEX BIB ₇ 1016_for	CCGGATCCATGGGCTACAAATTCAACGCCCCAG
pGEX BIB ₇ 1017_for	CCGGATCCATGTACAAATTCAACGCCCCAGTCGTG
pGEX BIB ₇ 1018_for	CCGGATCCATGAAATTCAACGCCCCAGTCGTGCC
pGEX BIB ₇ 1019_for	CCGGATCCATGTTCAACGCCCCAGTCGTGCCAAG
pGEX BIB ₇ 1020_for	CCGGATCCATGAACGCCCCAGTCGTGCCAAGTACG
pGEX BIB ₇ 1025_for	CCGGATCCATGCCAAGTACGTTTAATTTTCGGC
pGEX BIB ₇ 1038_rev	GGCTCGAGTTAATTCATTCTGGG
pGEX BIB ₇ 1033_rev	GGCTCGAGTTACGGGTTGCCGAAATTAAACGTAC
pGEX BIB ₇ 1032_rev	GCCTCGAGTTAGTTGCCGAAATTAAACGTACTTGG
pGEX BIB ₇ 1031_rev	GCCTCGAGTTAGCCGAAATTAAACGTACTTGGCAC
pGEX BIB ₇ 1030_rev	GCCTCGAG TTAGAAATTAAACGTACTTGGCACGAC
pGEX BIB ₇ 1029_rev	GGCTCGAGTTAATTAAACGTACTTGGCACGAC
pGEX BIB ₇ 1026_rev	GGCTCGAGTTAACTTGGCACGACTGGGGCGTT
by primer annealing:	
pGEX BIB ₇ 1025_for	GATCCATGCCAAGTACGTTTAATTTTCGGCAACCCGTAAC
pGEX BIB ₇ 1033_rev	TCGAGTTACGGGTTGCCGAAATTAAACGTACTTGGCATG
distance linker GST-NIB	
pGEX GST-Linker_for	GATCCGGTGGCGGTAGCGGTGGCGGCACCGGTGGCGGTAGCGGTG
pGEX GST-Linker_rev	GATCCACCGCTACCGCCACCGGTGCCGCCACCGCTACCGCCACCG

Table S2: Primers used to create the respective point mutations of GST-Imp7-NIB. Related to STAR Methods.

Sequencing:

pGEX_for	GGGCTGGCAAGCCACGTTTGGTG
pGEX_rev	CCGGGAGCTGCATGTGTAAGAGG

Neg. control

GST-M (f)	GATCCATGTGACCCGGGC
GST-M (r)	TCGAGCCCGGGTCACATG

Point mutations (in BIB 1002-1038):

pGEX BIB ₇ K1009E_for	GCACATGAATCCGAAATGATCGAGAAACAC
pGEX BIB ₇ K1009E_rev	GTGTTTCTCGATCATTTCCGATTTCATGTGC
pGEX BIB ₇ K1013E_for	TCCAAAATGATCGAGGAACACGGAGGCTAC
pGEX BIB ₇ K1013E_rev	GTAGCCTCCGTGTTCCCTCGATCATTTTGGA
pGEX BIB ₇ G1016S_for	GATCGAGAAACACGGATCCTACAAATTCAACGCC
pGEX BIB ₇ G1016S_rev	GGCGTTGAATTTGTAGGATCCGTGTTTCTCGATC
pGEX BIB ₇ Y1017G_for	GAGAAACACGGAGGCGGCAAATTCAACGCCCC
pGEX BIB ₇ Y1017G_rev	GGGGCGTTGAATTTGCCGCCTCCGTGTTTCTC
pGEX BIB ₇ Y1017F_for	GAGAAACACGGAGGCTTCAAATTCAACGCCCC
pGEX BIB ₇ Y1017F_rev	GGGGCGTTGAATTTGAAGCCTCCGTGTTTCTC
pGEX BIB ₇ 7Y1017S_for	GAGAAACACGGAGGCAGCAAATTCAACGCCCC
pGEX BIB ₇ 7Y1017Srev:	GGGGCGTTGAATTTGCTGCCTCCGTGTTTCTC
pGEX BIB ₇ K1018E_for	GAAACACGGAGGCTACGAATTCAACGCCCCAG
pGEX BIB ₇ K1018E_rev	CTGGGGCGTTGAATTCGTAGCCTCCGTGTTTC
pGEX BIB ₇ K1018G_for	GAAACACGGAGGCTACGGATTCAACGCCCCAG
pGEX BIB ₇ K1018G_rev	CTGGGGCGTTGAATCCGTAGCCTCCGTGTTTC
pGEX BIB ₇ C10 K1018E_for	GATCCATGGGAGGCTACGAATTCAACGCCCCAG
pGEX BIB ₇ C10 K1018E_rev	CTGGGGCGTTGAATTCGTAGCCTCCCATGGATC
pGEX BIB ₇ C10 K1018G_for	GATCCATGGGAGGCTACGGATTCAACGCCCCAG
pGEX BIB ₇ C10 K1018G_rev	CTGGGGCGTTGAATCCGTAGCCTCCCATGGATC
pGEX BIB ₇ F1019G_for	CACGGAGGCTACAAAGGCAACGCCCCAGTCGTG
pGEX BIB ₇ F1019G_rev	CACGACTGGGGCGTTGCCTTTGTAGCCTCCGTG
pGEX BIB ₇ F1019Y_for	CACGGAGGCTACAAATACAACGCCCCAGTCGTG
pGEX BIB ₇ F1019Y_rev	CACGACTGGGGCGTTGTATTTGTAGCCTCCGTG
pGEX BIB ₇ F1019S_for	CACGGAGGCTACAAAAGCAACGCCCCAGTCGTG
pGEX BIB ₇ F1019S_rev:	CACGACTGGGGCGTTGCTTTTGTAGCCTCCGTG
pGEX BIB ₇ FY1017/9S_for	GAAACACGGAGGCAGCAAAAAGCAACGCCCCAGTCG
pGEX BIB ₇ FY1017/9S_rev	CGACTGGGGCGTTGCTTTTGTGCTGCCTCCGTGTTTC
pGEX BIB ₇ Y17F19G_for	GAGAAACACGGAGGCGGCAAAGGCAACGCCCCAGTCGTG
pGEX BIB ₇ Y17F19G_rev	CACGACTGGGGCGTTGCCTTTGCCGCCTCCGTGTTTCTC
pGEX BIB ₇ YF17/19FY_for	GAGAAACACGGAGGCTTCAAATACAACGCCCCAGTCGTG
pGEX BIB ₇ YF17/19FY_rev	CACGACTGGGGCGTTGTATTTGAAGCCTCCGTGTTTCTC
pGEX BIB ₇ N1020S_for	GGAGGCTACAAATTCTCCGCCCCAGTCGTGCCAAG
pGEX BIB ₇ N1020S_rev	CTTGGCACGACTGGGGCGGAGAATTTGTAGCCTCC

Table S2: Primers used to create the respective point mutations of GST-Imp7-NIB. Related to STAR Methods.
(continued)

pGEX BIB ₇ V1024G_for	TTCAACGCCCCAGTCGGGCCAAGTACGTTTAAAT
pGEX BIB ₇ V1024G_rev	ATTAAACGTACTTGGCCCCGACTGGGGCGTTGAA
pGEX BIB ₇ V1024E_for	CAAATTCAACGCCCCAGTCGAGCCAAGTACGTTTAAATTTTCG
pGEX BIB ₇ V1024E_rev	CGAAATTAAACGTACTTGGCTCGACTGGGGCGTTGAATTTG
pGEX BIB ₇ V1024K_for	TTCAACGCCCCAGTCAACCCAAGTACGTTTAAAT
pGEX BIB ₇ V1024K_rev	ATTAAACGTACTTGGGTTGACTGGGGCGTTGAA
pGEX BIB ₇ P1025G_for	GCCCCAGTCGTGGGAAGTACGTTTAAATTTTCG
pGEX BIB ₇ P1025G_rev	CGAAATTAAACGTACTTCCCACGACTGGGGC
pGEX BIB ₇ F1028S_for	TGCCAAGTACGTCTAATTTTCGGCAA
pGEX BIB ₇ F1028S_rev	TTGCCGAAAATTAGACGTACTTGGCA
pGEX BIB ₇ F1028G_for	GTGCCAAGTACGGGTAAATTTTCGGCAACCC
pGEX BIB ₇ F1028G_rev	GGGTTGCCGAAAATTACCCGTACTTGGCAC
pGEX BIB ₇ F1028Y_for	GTGCCAAGTACGTATAATTTTCGGCAACCC
pGEX BIB ₇ F1028Y_rev	GGGTTGCCGAAAATTATACGTACTTGGCAC
pGEX BIB ₇ N1029G_for	GTCGTGCCAAGTACGTTTGGATTTCGGCAACCCGGCC
pGEX BIB ₇ N1029G_rev	GGCCGGGTTGCCGAATCCAAACGTACTTGGCACGAC
pGEX BIB ₇ N1029S_for	GTCGTGCCAAGTACGTTTAGTTTTCGGCAACCCGGCC
pGEX BIB ₇ N1029S_rev	GGCCGGGTTGCCGAAACTAAACGTACTTGGCACGAC
pGEX BIB ₇ F1030S_for	GTACGTTTAAATTCGGCAACCCGGC
pGEX BIB ₇ F1030S_rev	GCCGGGTTGCCGGAATTAAACGTAC
pGEX BIB ₇ F1030G_for	GTACGTTTAAATGGCGGCAACCCGGC
pGEX BIB ₇ F1030G_rev	GCCGGGTTGCCGCCATTAAACGTAC
pGEX BIB ₇ F1030Y_for	GTCGTGCCAAGTACGTTCAATTACGGCAACCCGGCCCCA
pGEX BIB ₇ F1030Y_rev	TGGGGCCGGGTTGCCGTAATTGAACGTACTTGGCACGAC
pGEX BIB ₇ G1031P_for	GTCGTGCCAAGTACGTTCAATTACCCAAACCCGGC
pGEX BIB ₇ G1031P_rev	GCCGGGTTTGGGTAATTGAACGTACTTGGCACGAC
pGEX BIB ₇ G1031I_for	GTCGTGCCAAGTACGTTCAATTACATCAACCCGGC
pGEX BIB ₇ G1031I_rev	GCCGGGTTGATGTAATTGAACGTACTTGGCACGAC
pGEX BIB ₇ N1032G_for	TGCCAAGTACGTCTAATTCGGCAACCCGG
pGEX BIB ₇ N1032G_rev	CCGGGTTGCCGGAATTAGACGTACTTGGCA

Table S5. X-link distances between the different residues of H1.0 from human, Imp7 and Impβ (Related to Figure 2). X link distances were determined and calculated as described in M&M. The Impβ:Imp7:H1.0-hs^{AF3} predicted model (column 5) as well as the revised structural model (column 6) were used. The last column (7) lists the Ca-Ca measured distance differences between columns 5 and 6, positive values indicate an increase of the distance and negative values a decrease of distance.

Protein 1	Residue nr.	Protein 2	Residue nr.	Ca-Ca distance [Å] (AF3 model)	Ca-Ca distance [Å] (revised structure)	Distance difference [Å]
H1.0-hs	27	Imp7	119	22.24	19.28	2.96
H1.0-hs	52	Imp7	163	15.33	17.31	-1.98
H1.0-hs	59	Imp7	162	15.18	15.67	-0.49
H1.0-hs	59	Imp7	262	30.03	30.57	-0.54
H1.0-hs	82	ImpB	854	22.05	23.66	-1.62
H1.0-hs	97	Imp7	163	23.12	28.98	-5.86
H1.0-hs	97	ImpB	854	16.91	17.59	-0.69
H1.0-hs	102	Imp7	163	26.93	37.93	-10.99
Imp7	119	H1.0-hs	52	15.42	14.86	0.56
Imp7	119	H1.0-hs	55	12.7	11.65	1.06
Imp7	119	H1.0-hs	59	11.91	10.36	1.55
Imp7	119	H1.0-hs	97	34.5	34.86	-0.37
ImpB	211	H1.0-hs	125	42.77	57.54	-14.77
Imp7	259	H1.0-hs	59	29.76	29.66	0.1
Imp7	262	H1.0-hs	52	18.94	20.99	-2.05
Imp7	283	ImpB	873	17.04	14.41	2.63
Imp7	489	ImpB	541	20.41	15.82	4.6
ImpB	541	H1.0-hs	121	35.27	31.66	3.61
ImpB	541	H1.0-hs	125	33.75	22.62	11.13
Imp7	774	H1.0-hs	108	28.4	44.59	-16.18
ImpB	867	Imp7	405	15.49	17.81	-2.33
H1.0-hs	27	H1.0-hs	97	20.98	24.43	-3.45
H1.0-hs	59	H1.0-hs	73	21.53	21.72	-0.18
H1.0-hs	82	H1.0-hs	97	9.3	8.73	0.57
H1.0-hs	82	H1.0-hs	102	12.75	18.45	-5.7
H1.0-hs	82	H1.0-hs	103	13.15	20.54	-7.39
H1.0-hs	82	H1.0-hs	108	19.55	32.86	-13.31
H1.0-hs	82	H1.0-hs	112	19.52	29.39	-9.87
H1.0-hs	82	H1.0-hs	121	22.97	26.27	-3.3
H1.0-hs	82	H1.0-hs	122	25.95	29.89	-3.94
H1.0-hs	82	H1.0-hs	125	28.87	35.07	-6.2
H1.0-hs	97	H1.0-hs	103	11.49	17.2	-5.71
H1.0-hs	97	H1.0-hs	116	21.95	24.22	-2.27
H1.0-hs	97	H1.0-hs	125	26.97	34.34	-7.37
H1.0-hs	102	H1.0-hs	108	13.22	17.41	-4.19
H1.0-hs	102	H1.0-hs	112	14.79	16.09	-1.3
H1.0-hs	108	H1.0-hs	112	7.47	6.3	1.18
H1.0-hs	108	H1.0-hs	115	11.74	10.44	1.3
H1.0-hs	109	H1.0-hs	115	10.06	9.7	0.36
H1.0-hs	112	H1.0-hs	121	12.75	12.67	0.08
H1.0-hs	116	H1.0-hs	112	6	6.11	-0.12
Imp7	119	Imp7	162	11.72	9.4	2.31
Imp7	119	Imp7	163	14.91	12.17	2.75
H1.0-hs	121	H1.0-hs	125	9.89	11.24	-1.36
Imp7	259	Imp7	262	4.93	5.02	-0.09
Imp7	306	Imp7	314	12.6	11.63	0.97
Imp7	405	Imp7	447	15.36	16.72	-1.37
Imp7	429	Imp7	314	20.47	21.11	-0.65
Imp7	750	Imp7	968	23.53	21.63	1.91
ImpB	859	ImpB	873	21.15	20.48	0.67
ImpB	867	ImpB	857	15.5	15.31	0.19
ImpB	867	ImpB	873	9.78	9.82	-0.04
Imp7	968	Imp7	312	91.56	98.32	-6.76

Only non-ambiguous cross-links are listed.

Table S7: Average binding statistics of ITC experiments. The effect on various point mutations within the conserved residues of the NIB of Imp7 are shown, emphasizing the importance of the aromatic residues (Related to Figure 5). The averaged experimental results (N) are presented, with correlated plots available in Supplementary Figures S14 - S17.

	N	KD [μ M]	SD (μ M)	Δ H	SD (kJ/mol)	T Δ S	SD (kJ/mol)	Δ G	SD (kJ/mol)
1002-1038	19	0,3	0,2	-69,6	15,9	22,5	2,8	-37	1,4
K1009E	3	0,6	0,16	-44,7	2,1	9,6	2,6	-35	0,64
K1013E	3	0,61	0,09	-49,2	3,2	14,3	3,7	-34,9	0,4
G1015P	1	0,19	n.d.	-58,9	n.d.	19,2	n.d.	-39,8	n.d.
G1015S	3	0,09	0,04	-59	2,5	19,2	3,5	-39,8	1,1
GG15/16SS	2	1,16	0,32	-48,8	12,2	15,4	12,9	-33,4	0,7
GG15/16PP	2	0,4	0,07	-49,6	0,3	13,8	0,7	-35,9	0,6
G1016P	1	0,19	n.d.	-44,6	n.d.	6,88	n.d.	-37,7	n.d.
G1016S	4	1,23	0,32	-61,1	7,8	27,9	8,4	-33,2	0,7
Y1017S	2	no binding							
Y1017G	2	no binding							
Y1017F	6	0,3	0,08	-69,5	10,8	32,8	11,2	-36,7	0,7
K1018E	16	1,41	0,73	-59,2	20,3	37,2	27	-33,2	1,1
K1018G	12	1,43	0,59	-70,3	27,1	37,1 1	17	-33,2	1,1
F1019Y	16	1,36	0,32	-64,7	21,1	31,6	21	-33	0,6
F1019G	3	no binding							
F1019S	4	no binding							
YF17/19FY	4	3,8	1,1	-68,2	16,7	37,7	16,7	-30,6	0,8
N1020S	4	0,16	0,05	-70,4	5,8	32,1	5,2	-38,3	0,7
V1024E	3	4,66	2,18	-48,8	18,8	18,6	19	-30,9	1,2
V1024T	10	1,11	0,6	-63,9	16,4	30,1 4	15,5	-33,7	1,3
P1025G	6	2,02	1,5	-63,1	14,3	30,7	4,6	-32,4	1,4
F1028G	2	no binding							
F1028S	11	no binding							
F1028Y	4	1,72	0,88	-49	12,9	16,4	14,1	-32,6	1,2
N1029S	5	0,17	0,03	-71,2	8,9	33,2	9	-38	0,4
F1030G	3	no binding							
F1030S	8	no binding							
F1030Y	8	20,9	27	-41	16,9	14,9	16,8	-28,7	4
FF28/30SS	5	no binding							
FF28/30YY	3	no binding							
G1031P	3	0,31	0,14	-80,4	27	43,5	27,8	-36,8	1,22
G1031I	5	0,44	0,07	-54,5	8,4	18,7	8,7	-35,7	0,4
N1032G	3	0,16	0,02	82,1	9,4	44	9,2	-38,1	0,3